P517007.PDF [Page: 3 of 54]

Copy No. 33

DEFENCE R&D DÉFENSE

Computation of Fracture Toughness of Giant Magnetostrictive Material

T.S. Koko, P.A. Rushton and M.E. Norwood

Martec Limited
400-1888 Brunswick Street
Halifax, N.S.
B3J 3J8

SECURITY CAUTION
THIS PUBLICATION CONTAINS CLASSIFIED INFORMATION AFFECTING THE DEFENCE OF CANADA, AND SHALL BE PROTECTED IN ACCORDANCE WITH THE REGULATIONS APPEARING HEREON. RELEASE OF THIS PUBLICATION, OR INFORMATION CONTAINED HEREIN, TO ANY PERSON NOT AUTHORIZED TO RECEIVE IT, IS PROHIBITED BY THE OFFICIAL SECRETS ACT.

Contract #W7707-008853/WIHAL

Defence R&D Canada

Contractor Report
DREA CR 2001-090
May 2001

National Defence Défense nationale

Canada

P517007.PDF [Page: 4 of 54]

REPRODUCTION QUALITY NOTICE

This document is the best quality available. The copy furnished to DRDCIM contained pages that may have the following quality problems:

: Pages smaller or Larger than normal

: Pages with background colour or light coloured printing

: Pages with small type or poor printing; and or

: Pages with continuous tone material or colour photographs

Due to various output media available these conditions may or may not cause poor legibility in the hardcopy output you receive.

☒ If this block is checked, the copy furnished to DRDCIM contained pages with colour printing, that when reproduced in Black and White, may change detail of the original copy.

P517007.PDF [Page: 5 of 54]

104-06991/

Copy No: _____

COMPUTATION OF FRACTURE TOUGHNESS OF GIANT MAGNETOSTRICTIVE MATERIAL

T. S. Koko, P. A. Rushton, and M. E. Norwood

Martec Limited
400-1888 Brunswick Street
Halifax, NS
B3J 3J8

SECURITY CAUTION

THIS PUBLICATION CONTAINS CLASSIFIED INFORMATION AFFECTING THE DEFENCE OF CANADA, AND SHALL BE PROTECTED IN ACCORDANCE WITH THE REGULATIONS APPEARING HEREON. RELEASE OF THIS PUBLICATION, OR INFORMATION CONTAINED HEREIN, TO ANY PERSON NOT AUTHORIZED TO RECEIVE IT, IS PROHIBITED BY THE OFFICIAL SECRETS ACT.

Contract # W7707-008853/WIHAL

Defence Research Establishment Atlantic

Contractor Report

DREA CR 2001-090

May 2001

P517007.PDF [Page: 6 of 54]

Authors

T. S. Koko, P. A. Rushton, M. E. Norwood, Martec Limited

Approved by

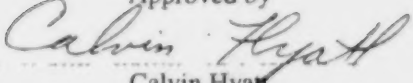

Calvin Hyatt

Defence Scientist

Approved for release by

Kirk Foster

Chair Document Review Panel

© Her Majesty the Queen as represented by the Minister of National Defence, 2001

© Sa majesté la reine, représentée par le ministre de la Défense nationale, 2001

P517007.PDF [Page: 7 of 54]

Abstract

Magnetostrictive materials such as Etrema Terfenol-D are classified as smart materials, which, when subjected to a magnetic field, experience internal strains, and conversely, when subjected to mechanical strains, experience a magnetic field. The most limiting factor impeding the use of magnetostrictive materials lies in their inherent susceptibility to brittle fracture. Previous studies at DREA have led to the development of a new mechanical device for mode II fracture testing of magnetostrictive materials in the presence or absence of a magnetic field. The test specimen is cylindrical in shape, 6.35 mm in diameter, 25.4 mm in length, with a 20 μm wide EDM notch extending through its diameter for a distance of 6.35 mm along its length. The present study applies finite element technology to support these experimental investigations, thereby lending assistance in the assessment of mode II fracture toughness for magnetostrictive materials. This is an initial exploratory effort, in which the fully coupled non-linear behavior of the material is not considered. Rather, a methodology for converting the applied magnetic field to an equivalent mechanical load, based on the material's magnetostrictive properties, is devised and applied.

The DSA-VAST finite element software was employed to produce a model comprised of conventional solid elements, and also featuring DSA's enriched twenty-noded solid fracture element. Two load cases were investigated, namely one in which a mechanical load was applied to the specimen in the absence of a magnetic field, and a second case in which a magnetic field was applied to the specimen in addition to a mechanical load. In the absence of an applied magnetic field, the mode II fracture toughness was found to be approximately 4.497 MPa$\sqrt{m}$, which is in the range of values reported for ceramic-like materials. On the other hand, in the presence of an applied magnetic field (simulated by an equivalent compressive prestress), the resulting mode II fracture toughness was found to be 2.768 MPa$\sqrt{m}$, a 39% reduction from the corresponding 'zero-field' value. In each laod case, the out-of-plane displacements were more than twice the axial displacements, thereby suggesting that additional support be placed along the longitudinal boundaries of the specimen in order to attain a more accurate assessment of mode II fracture toughness.

17007 PDF [Page: 8 of 54]

Resume

Les matériaux magnétostrictifs tels que le Terfenol-D d'Etrema sont classés parmi les matériaux intelligents, lesquels subissent des déformations internes lorsqu'ils sont soumis à un champ magnétique, et, réciproquement, induisent un champ magnétique lorsqu'ils sont soumis à des déformations mécaniques. Le facteur qui limite le plus l'emploi des matériaux magnétostrictifs est leur sensibilité naturelle à la rupture fragile. Lors d'études antérieures réalisées au CRDA, on a mis au point un nouveau dispositif mécanique qui permet d'effectuer des essais de rupture de mode II de matériaux magnétostrictifs, en présence ou non d'un champ magnétique. L'éprouvette cylindrique, d'un diamètre de 6,35 mm et d'une longueur de 25,4 mm, possède une entaille d'une largeur de 20 µm, usinée par décharge électronique (EDM), qui se prolonge, suivant le diamètre, sur une distance de 6,35 mm, parallèlement à sa longueur. Au cours de la présente étude, on a appliqué la technique des éléments finis lors des expériences en question afin de faciliter l'évaluation de la ténacité à la rupture de mode II des matériaux magnétostrictifs. On ne tient pas compte, pour ces travaux préliminaires, du comportement non-linéaire à couplage global du matériau. On a plutôt élaboré et appliqué une méthode permettant de convertir le champ magnétique appliqué en une valeur équivalente de charge mécanique, en se basant sur les propriétés magnétostrictives du matériau.

On a utilisé le logiciel d'analyse par éléments finis DSA-VAST pour générer un modèle constitué d'éléments solides classiques et comportant aussi l'élément DSA renforcé, à vingt nœuds, pour modéliser la rupture d'un solide. On a étudié deux cas de charge, soit un premier pour lequel l'échantillon est soumis à une charge mécanique, en l'absence de champ magnétique, et un second, pour lequel l'échantillon est soumis à un champ magnétique, en plus de la charge mécanique. On a observé qu'en l'absence de champ magnétique, la ténacité à la rupture de mode II est d'environ 4,497 MPa$\sqrt{m}$, une valeur qui se situe dans le domaine de celles observées pour les matériaux de nature céramique. D'autre part, on a observé qu'en présence d'un champ magnétique (la simulation de l'application d'un tel champ a été effectuée en exerçant une précontrainte en compression équivalente), la ténacité à la rupture de mode II est de 2,768 MPa$\sqrt{m}$, soit une diminution de 39 % par rapport à la valeur « à champ nul » correspondante. Dans les deux cas de charge, les valeurs des déplacements hors-plan étaient plus de deux fois supérieures à celles des déplacements axiaux, ce qui suggère qu'il faudrait installer des supports additionnels le long des bords longitudinaux de l'échantillon afin d'obtenir une meilleure évaluation de la ténacité à la rupture de mode II.

P517007 PDF [Page: 9 of 54]

This page intentionally left blank.

P517007.PDF [Page: 10 of 54]

Executive summary

Introduction: Magnetostrictive materials such as TERFENOL-D have great promise for use in sonar and other devices because they provide a high force high elongation transducer in a compact low voltage package. They are limited though by poor toughness. Design of improved alloys and utilization of existing alloys requires improved toughness assessment techniques. In this report, a finite element model of a toughness test to assess fracture toughness of TERFENOL-D is presented.

Significance of Results: These are the first reported measurements of TERFENOL-D toughness. The finite element calculations reported here allowed toughness values to be determined from previous experiments. The results show that there is an unexpectedly large amount of mode III crack growth in a specimen thought to give mostly mode II loading.

Principal Results: Approximate values of mode II fracture toughness were determined.

Koko, T. S., Rushton, P. A., and Norwood, M. E. 2001
Computation of Fracture Toughness of Giant Magnetostrictive Material
DREA CR 2001-090
Martec Limited

P517007.PDF [Page: 11 of 54]

Sommaire

Introduction: Les matériaux magnétostrictifs tels que le TERFENOL-D sont très prometteurs, en matière d'utilisation dans les sonars et autres dispositifs, car ils constituent des transducteurs à force et à allongement élevés, dans un ensemble compact à basse tension électrique. Leur ténacité médiocre limite toutefois leurs applications. La conception d'alliages améliorés et l'utilisation des alliages existants exigent des méthodes d'essai améliorées pour évaluer la ténacité de ces matériaux. Le présent rapport contient un modèle à éléments finis d'un essai de ténacité permettant de déterminer la ténacité à la rupture du TERFENOL-D.

Importance des résultats: Les résultats du présent rapport constituent les premières mesures publiées relatives à la ténacité du TERFENOL-D. Les calculs par éléments finis utilisés ont permis de déterminer les valeurs de ténacité à partir d'expériences antérieures. Les résultats démontrent qu'il existe une proportion de propagation des fissures de mode III d'une ampleur imprévue, et ce, dans un échantillon qu'on considère comme possédant surtout des caractéristiques de chargement de mode II.

Principaux résultats: On a déterminé des valeurs approximatives de la ténacité à la rupture de mode II.

Koko, T. S., Rushton, P. A., et Norwood, M. E., 2001
Calcul de la ténacité à la rupture de matériaux à magnétorésistance géante
Martec Limited
DREA CR 2001-090

517007.PDF [Page: 12 of 54]

ACKNOWLEDGEMENTS

We would like to kindly acknowledge the assistance of Dr. Calvin Hyatt of the Dockyard Lab at Defence Research Establishment Atlantic in Halifax, Nova Scotia.

P517007.PDF [Page: 13 of 54]

TABLE OF CONTENTS

ABSTRACT ii
ACKNOWLEDGEMENTS iii
TABLE OF CONTENTS iv
LIST OF FIGURES v
LIST OF TABLES vi
INTRODUCTION 1-1
1.1 Background and Objectives of Study 1-1
1.2 Layout of Report 1-2
2. PROBLEM DESCRIPTION 2-1
2.1 Specimen Configurations 2-1
2.2 Requirements 2-1
3. FINITE ELEMENT METHODOLOGY 3-1
3.1 Approach and Assumptions 3-1
3.2 Finite Element Modeling 3-1
3.3 Constitutive Relations for Magnetostrictive Materials 3-2
3.4 Boundary Conditions 3-5
3.5 Applied Loading 3-5
3.5.1 In the Absence of a Magnetic Field 3-5
3.5.2 In the Presence of an Applied Magnetic Field 3-6
4. RESULTS AND DISCUSSIONS 4-1
4.1 Specimen Response in the Absence of an Applied Magnetic Field 4-1
4.2 Specimen Response in the Presence of an Applied Magnetic Field 4-2
5. SUMMARY, CONCLUSIONS, AND RECOMMENDATIONS 5-1
5.1 Summary and Conclusions 5-1
5.2 Recommendations 5-2
6. REFERENCES 6-1

P517007.PDF [Page: 14 of 54]

LIST OF FIGURES

Figure 2.1 - Device for measuring mode II fracture toughness 2-3
Figure 2.2 - Configuration of test specimen 2-4
Figure 3.1 - Sectional view of specimen illustrating crack lines, crack tips, and enriched fracture elements 3-8
Figure 3.2 - Typical curves of (a) Flux density (B) versus field (H), (b) Strain (S) versus flux density (B), and (c) Strain (S) versus field (H) for magnetostrictive materials 3-8
Figure 3.3 - Fixed boundary conditions applied to far end of specimen 3-9
Figure 3.4 - Applied pressure loading (scale factor, $\phi = 294$) 3-9
Figure 3.5 - Applied pressure loading simulating applied magnetic field and mechanical loading 3-10
Figure 4.1 - Mesh discretization for (a) model R0, (b) model R1, (c) model R2, and (d) model R3 4-6
Figure 4.2 - Displacement contours for (a) X-, (b) Y-, and (c) Z-translation (no magnetic field applied) 4-7
Figure 4.3 - Stress components in the (a) X-direction, (b) Y-direction, and (c) Z-direction (no magnetic field applied) 4-8
Figure 4.4 - VonMises stress contours for model R2 (no magnetic field applied) 4-9
Figure 4.5 - Mode I stress intensity factor for model R2 (no magnetic field applied) 4-9
Figure 4.6 - Stress intensity factors for (a) mode I, (b) mode II, and (c) mode III fracture (no magnetic field applied, only enriched fracture elements shown) 4-10
Figure 4.7 - Displacement contours for (a) X-, (b) Y-, and (c) Z-translation (57.6 kA/m magnetic field applied) 4-11
Figure 4.8 - Axial stress components (57.6 kA/m magnetic field applied) 4-12
Figure 4.9 - VonMises stress contours (57.6 kA/m magnetic field applied) 4-12
Figure 4.10 - Magnetostrictive stress intensity factors for (a) Mode I, (b) Mode II, and (c) Mode III fracture (57.6 kA/m magnetic field applied, only enriched fracture elements shown) 4-14

P517007.PDF [Page: 15 of 54]

LIST OF TABLES

Table 2.1 - Specimen dimensions 2-3
Table 3.1 - Magnetostrictive material properties for test specimens 2 and 4 (Terfenol-D)..... 3-7
Table 4.1 - Summary of convergence study on FE mesh density..... 4-5
Table 5.1 – Summary of results from linear elastic FE analysis 5-4

P517007.PDF [Page: 16 of 54]

1. INTRODUCTION

1.1 Background and Objectives of Study

Magnetostrictive materials are a class of smart materials, which, when subjected to a magnetic field, undergo domain changes that cause internal strains in the material, and conversely, when subjected to mechanical strain, produce a magnetic field in the material. Due to their large strain capabilities, these materials are increasingly being considered for demanding applications such as active noise damping, sonar devices and reactive structures. The most commonly used magnetostrictive material is Terfenol-D. However, one of the factors limiting the use of such materials is their brittleness, which renders them susceptible to brittle fracture. DREA has been conducting experimental investigations on the fracture behavior of these materials. These studies have led to the development of a new mechanical device for mode II fracture testing of magnetostrictive materials in the presence or absence of a magnetic field [1].

A typical test specimen [1] is cylindrical in shape, 25.4 mm in length, and 6.35 mm in diameter, with a 20μ wide EDM notch extending through its diameter for a distance of 6.35 mm along its length. The mechanism for mechanical loading consists of two loading pins: an upper circular pin and a lower semicircular pin. While the circular pin transfers a compressive force to the entire face of the unnotched end of the specimen, the semicircular pin transfers a compressive force to only one-half of the notched end of the specimen. This loading generates an in-plane shear, which at the crack front is the driving force for mode II crack advance.

The purpose of this study is to apply finite element technology to support the experimental investigations related to the measurement of mode II fracture toughness of the material. This is an initial effort to provide rough estimates of the mode II fracture toughness. Hence, the fully coupled non-linear behavior of the material will not be considered in this study. Rather, a methodology for converting the applied magnetic field to an equivalent mechanical load, based on the material's coupling properties, is devised and applied.

P517007.PDF [Page: 17 of 54]

1.2 Layout of Report

Chapter 2 provides detailed descriptions of the specimen configurations considered in this study. The finite element methodology utilized in the investigation is presented in Chapter 3, which includes details of the finite element meshes, constitutive material models, boundary and loading conditions, and the solution methodology. The finite element results are presented in Chapter 4, along with discussions of the results. Finally, Chapter 5 provides a summary of the study and the conclusions reached.

P517007.PDF [Page: 18 of 54]

2. PROBLEM DESCRIPTION

2.1 Specimen Configurations

The device used for measuring the mode II fracture toughness of the magnetostrictive material is illustrated in Figure 2.1. A detailed description of the device has been provided by Cunningham et al [1]. Figure 2.2 shows a schematic representation of the specimen. The specimen is cylindrical in shape, with a diameter of 6.35 mm and a length of 25.4 mm, as summarized in Table 2.1. An EDM notch, 20 μm in width and 6.35 mm in length, has been cut parallel to the specimen as shown. The mechanism for mechanical loading consists of two loading pins: an upper circular pin and a lower semicircular pin. The circular pin applies compressive force to the face of the unnotched end of the specimen, while the semicircular pin applies compressive force to only one-half of the notched end of the specimen. This loading generates in-plane shear, which induces mode II crack advance [1]. However, it should be noted that because the applied loads at each end of the specimen are not co-linear, the specimen experiences some out-of-plane bending, which could cause crack advance in mode I or III. By imposing a magnetic field on the specimen, parallel to the loading axis, the crack-driving force can also be increased. Due to magnetostriction, an applied magnetic field causes the strain in the unconstrained portion to increase more than that in the constrained portion, thereby augmenting the mechanical mode II fracture mechanism.

2.2 Requirements

Under the present investigation, the following tasks will be performed:

(a) Define the finite element approach for modeling the mode II fracture toughness of magnetostrictive material in the presence or absence of a magnetic field.

(b) Compute the mode II fracture toughness of the magnetostrictive material specimen with no applied magnetic field.

P517007.PDF [Page: 19 of 54]

(c) Compute the mode II fracture toughness of the magnetostrictive material specimen when subjected to both a mechanical load and an applied magnetic field.

(d) Compare the finite element results with experimental results and recommend improvements to the FE approach

Table 2.1 – Specimen dimensions [1]

Parameter	Value
Length (mm)	25.4
Diameter (mm)	6.35
EDM Notch Depth (mm)	0.02
EDM Notch Length (mm)	6.35

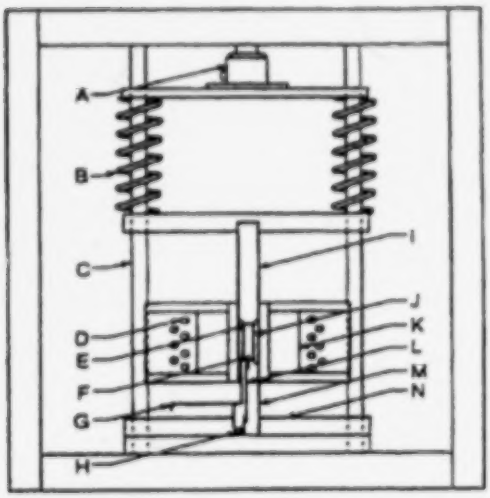

Figure 2.1 – Device for measuring mode II fracture toughness [1]

P517007.PDF [Page: 21 of 54]

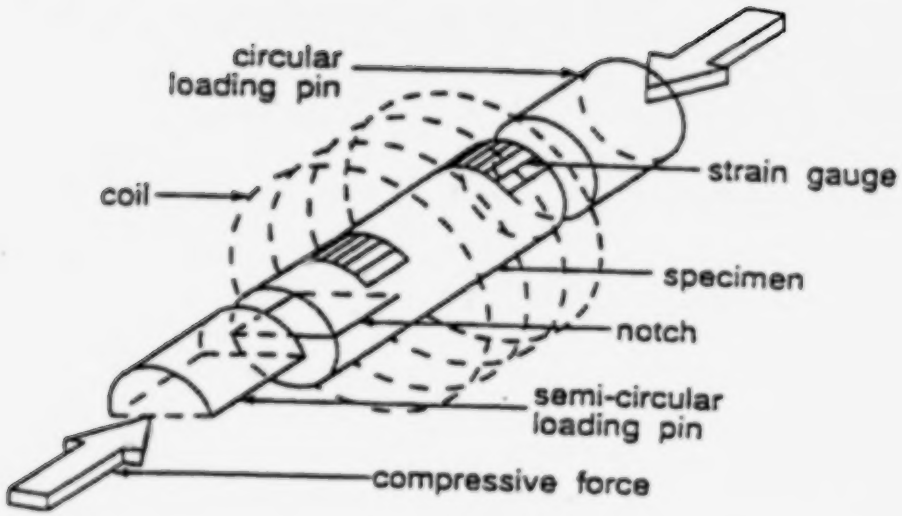

Figure 2.2 - Configuration of test specimen [1]

P517007.PDF [Page: 22 of 54]

3. FINITE ELEMENT METHODOLOGY

3.1 Approach and Assumptions

For the current investigation, it was assumed that the material behaves in the linear regime. The fully coupled nonlinear magnetostrictive behavior will not be considered here. For the purposes of a static finite element analysis, it was further assumed that the strains induced by a given magnetic field could be simulated by an equivalent mechanically applied load. The methodology for converting the applied magnetic field to an equivalent mechanical load, based on the material's coupling properties, will be discussed later in Section 3.3.

3.2 Finite Element Modeling

The DSA-VAST finite element software was used to model the fracture behavior of the magnetostrictive material specimen. Available within the DSA-VAST FE software is an enriched twenty-noded solid fracture element, which allows automatic computation of the crack front stress intensity factors for mode I, II, and III crack growth. Details of the finite element model are provided in the following paragraphs.

The finite element mesh was comprised of both conventional twenty-noded solid elements and DSA's enriched twenty-noded solid fracture element. A number of crack lines were employed to sufficiently define the through-diameter crack orientation. The corresponding crack front locations were characterized by creating crack tips at the appropriate extreme of each crack line. Elements in the immediate vicinity of each crack tip were then converted to enriched elements, such that these fracture elements completely surrounded the crack front. Figure 3.1 illustrates the finite element mesh used to model the fracture behavior of the magnetostrictive specimen. To differentiate the twenty-noded enriched fracture elements from the conventional solid elements, they have been colored light orange. The top left-hand section of the model has been removed to show more clearly the crack orientation and crack front location.

P517007.PDF [Page: 23 of 54]

3.3 Constitutive Relations for Magnetostrictive Materials

A magnetic field can be introduced into a ferrous material by passing an electric current through coils wound around the material. Magnetostriction is the result of a current-induced realignment of small magnetic domains within a magnetostrictive material. This realignment, in turn, induces internal strains in the material, which progressively increase until a saturation level is reached where all the magnetic domains have been realigned. If the direction of the current were reversed, the domains would also reverse until they are again aligned in the direction of the magnetic field. Rare earth magnetostrictive materials may produce strains up to 2000μ for a given magnetic field imposed by an electric current passed through a surrounding coil. Figure 3.2 shows typical magnetic flux density (B) versus magnetic field (H), strain versus magnetic flux density (B), and strain versus magnetic field (H) curves for magnetostriction. These plots help to illustrate the hysteresis effect on some magnetostrictive materials subjected to magnetic fields. For Terfenol-D, this effect is rather insignificant and can usually be neglected without appreciable error. In applications such as accurate positioning devices, the hysteresis effect may warrant more detailed consideration.

Butler [2] refers to magnetostriction as "a transduction process in which electrical energy is converted into mechanical energy, as in the case of actuators or sound projectors". Similarly, when operated in the linear regime, magnetostrictive materials are also capable of converting mechanical energy into electrical energy, as is the case for a variety of sensors and energy converters. Magnetostrictive materials are being considered for more demanding applications including active noise damping, sonar-related devices, and reactive structures. The fundamental transduction relations are given by Equations 3.1a and 3.2a below.

$$\varepsilon = \frac{T}{E^H} + d \cdot H \qquad [3.1a]$$

$$B = d \cdot T + \mu^T \cdot H \qquad [3.2a]$$

P517007.PDF [Page: 24 of 54]

Where ε = strain

T = mechanically applied stress

E^H = open-circuit elastic modulus (no magnetic field applied)

d = constant which yields a mechanical strain for a given magnetic field (i.e., the slope of the linear region of the strain versus magnetic field curve, Figure 3.2), or a magnetic flux density for a given mechanical stress

H = magnetic field

B = flux density

μ^T = stress-free permeability, corresponds to the initial slope of the flux density versus magnetic field (B vs H) hysteresis curve (recall Figure 3.2)

In the absence of an applied stress (i.e., T = 0), the above relations reduce to the following

$$\varepsilon = d \cdot H \qquad [3.1b]$$

$$B = \mu^T \cdot H \qquad [3.2b]$$

For a specimen of length L, around which N coils have been wound, the magnetic field (H) induced by a given current (I) may be calculated using Equation 3.3.

$$H = \left(\frac{N}{L}\right) \cdot I \qquad [3.3]$$

For open-circuit conditions, the current I = 0, and thus by Equation 3.3, H = 0. Consequently, Equations 3.1a and 3.2a reduce to

$$\varepsilon = \frac{T}{E^H} \qquad [3.1c]$$

$$B = d \cdot T \qquad [3.2c]$$

P517007.PDF [Page: 25 of 54]

On the other hand, for short-circuit conditions, the flux density B = 0, and Equation 3.2a yields a constant magnetic field given by

$$H = \frac{-d \cdot T}{\mu^T} \qquad [3.2d]$$

Rearranging Equation 3.2d yields a relation for the equivalent mechanical stress state based on an applied magnetic field and the magnetostrictive material properties.

$$T = \frac{-\mu^T \cdot H}{d} \qquad [3.2e]$$

The so-called 'coupling coefficient' (k) is a very significant parameter for a transducer. It is very useful, for example, in relating stress-free parameters to their strain-free equivalents, or likewise, in relating the open- and closed-circuit parameters. The square of the coupling coefficient (k^2) represents the ratio of the energy converted during a transduction process to the total energy stored. For example, a coupling coefficient of 1 indicates perfect transduction, meaning for all of the type 1 energy stored is converted to type 2 energy during transduction; therefore, the larger the k-value, the greater the transduction efficiency. The coupling coefficient, k, is given by the following relation [2]

$$k^2 = \frac{d^2 \cdot E^H}{\mu^T} \qquad [3.4]$$

For Terfenol-D, the coupling coefficient is approximately 0.72, which corresponds to a transduction efficiency of approximately 52%. A number of magnetostrictive parameters are related via the coupling coefficient. For example the strain-free (clamped) and stress-free (unclamped) permeabilities are related by

$$\mu^S = \mu^T \cdot \left(1 - k^2\right) \qquad [3.5]$$

P517007.PDF [Page: 26 of 54]

Similarly, the short-circuit compliance (C) is related to the open-circuit compliance by

$$C^B = C^H \cdot \left(1 - k^2\right) \qquad [3.6a]$$

Since compliance is simply the inverse of the elastic modulus, Equation 3.6a may also be written as

$$E^H = E^B \cdot \left(1 - k^2\right) \qquad [3.6b]$$

Note that the superscript 'S' represents the zero strain (i.e., 'clamped') condition, the superscript 'B' indicates zero flux or a short-circuit coil, the superscript 'H' denotes an open circuit, and the superscript 'T' indicates 'free' conditions. Typical magnetostrictive material properties for Terfenol-D are included in Table 3.1.

3.4 Boundary Conditions

To best simulate the support conditions existing in the experimental setup, the unnotched end of the specimen was assumed to be completely restrained from any translation or rotation about all three coordinate axes. The applied boundary conditions are illustrated in Figure 3.3.

3.5 Applied Loading

The applied loading will be discussed in the following subsections for the cases of zero magnetic field, and an applied magnetic field.

3.5.1 In the Absence of a Magnetic Field

The corresponding 'zero-field' elastic modulus was assumed to be 30,000 MPa. During experimental testing, a compressive force was mechanically applied to each magnetostrictive

P517007.PDF [Page: 27 of 54]

specimen of Terfenol-D by means of a semicircular pin placed over one half of the notched end of each specimen. For the purposes of FE modeling, this compressive force was simulated by an equivalent pressure applied to the axial (z-directed) face of each element in the top half of the specimen at its notched end. The applied loading conditions are illustrated in Figure 3.4. It should be noted that a scale factor of 294 was applied to the unit pressure illustrated, thereby equating the total applied load to the initial (experimental) failure load (474.6 kg = 4656 N) for specimen 4 of the experimental data set provided by Hyatt [3]. Material properties and loading conditions for specimen 4 have been included in Table 3.1. For additional information regarding the loading conditions and results obtained for all specimens tested, the report by Hyatt [3] should be consulted.

3.5.2 In the Presence of an Applied Magnetic Field

In this case, the applied magnetic field was simulated by means of a compressive prestress applied over the entire model cross-section at the notched end. The elastic modulus was assumed to be 60,000 MPa, an average value for conditions of zero flux density (i.e., constant magnetic field). Using Equations 3.2e and 3.5, in conjunction with appropriate material properties, applied current, and applied magnetic field data for specimen 2 (see Table 3.1) of the experimental data set provided in the report by Hyatt [3], the magnitude of this induced compressive prestress was calculated as approximately 21.5 MPa. In addition to this applied prestress, a compressive pressure of 181 MPa was applied in the same manner as in the previous load case. This value corresponds to the initial failure load (292 kg = 2865 N) for specimen 2 of the experimental data set included in Hyatt [3]. The applied loading conditions in the presence of an applied magnetic field are illustrated in Figure 3.5.

Table 3.1 – Magnetostrictive material properties for test specimens 2 and 4 (Terfenol-D) [2 & 3]

Material Property / Loading Condition	Specimen 4 (No Field)	Specimen 2 (H_{avg}=57.6 kA/m)
Density (Ns^2/mm^4)	$9.25x10^{-9}$	$9.25x10^{-9}$
Poisson Ratio	0.30	0.30
'd' Constant (m/A)	$15.0x10^{-9}$	$15.0x10^{-9}$
'g' Constant (T^{-1})	$1.28x10^{-3}$	$1.28x10^{-3}$
Coupling Coefficient 'k'	0.72	0.72
'Zero Field' Elastic Modulus, E^H (MPa)	$30.0x10^3$	N/A
'Zero Flux' Elastic Modulus, E^B (MPa)	N/A	$60.0x10^3$
Stress-Free Permeability, μ^T (Tm/A)	$9.2x4\pi x10^{-7}$	$9.2x4\pi x10^{-7}$
Strain-Free Permeability, μ^S (Tm/A)	$4.5x4\pi x10^{-7}$	$4.5x4\pi x10^{-7}$
Tensile Strength (MPa)	28	28
Compressive Strength (MPa)	700	700
Applied Electric Current, I (A)	N/A	5
Applied Magnetic Field, H (kA/m)	N/A	57.6
Experimental Fracture Load (kg) (Small Cracks at Notch)	494.6	292.0
Load at Possible Tensile Failure at Support (kg)	254.3	N/A
Magnetostriction	N/A	2000μ

P517007.PDF [Page: 29 of 54]

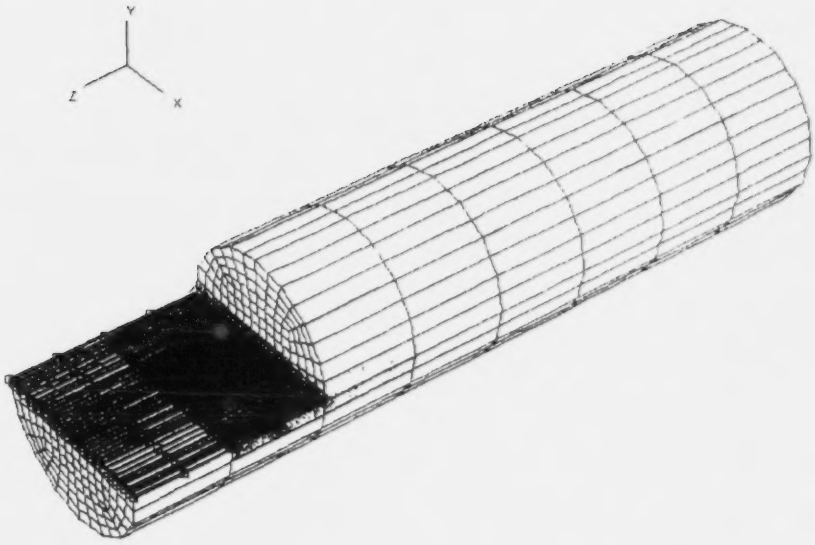

Figure 3.1 – Sectional view of specimen illustrating crack lines, crack tips, and enriched fracture elements

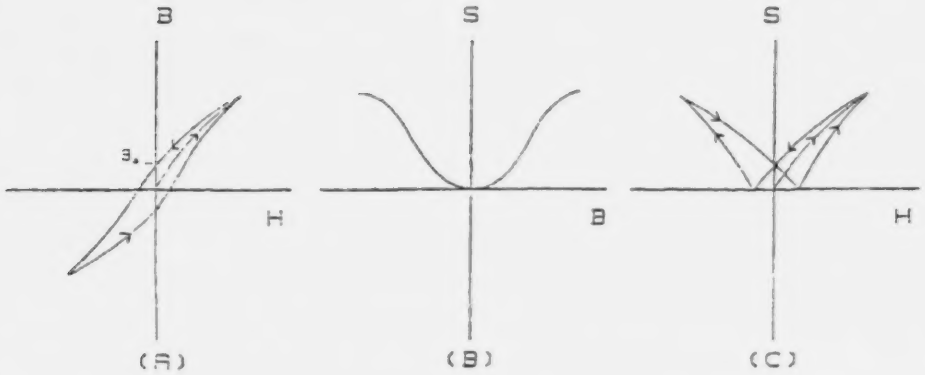

Figure 3.2 – Typical curves of (a) Flux density (B) versus field (H), (b) Strain (S) versus flux density (B), and (c) Strain (S) versus field (H) for magnetostrictive materials [2]

P517007.PDF [Page: 30 of 54]

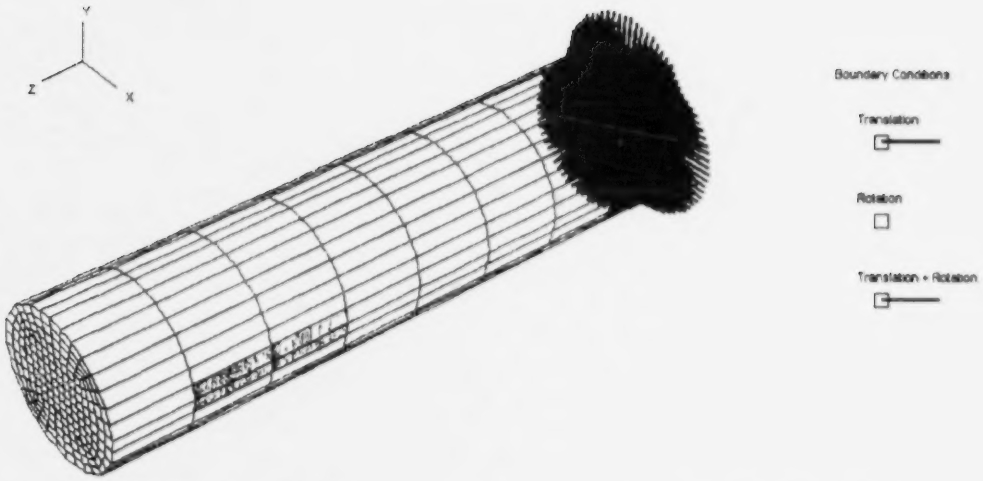

Figure 3.3 – Fixed boundary conditions applied to far end of specimen

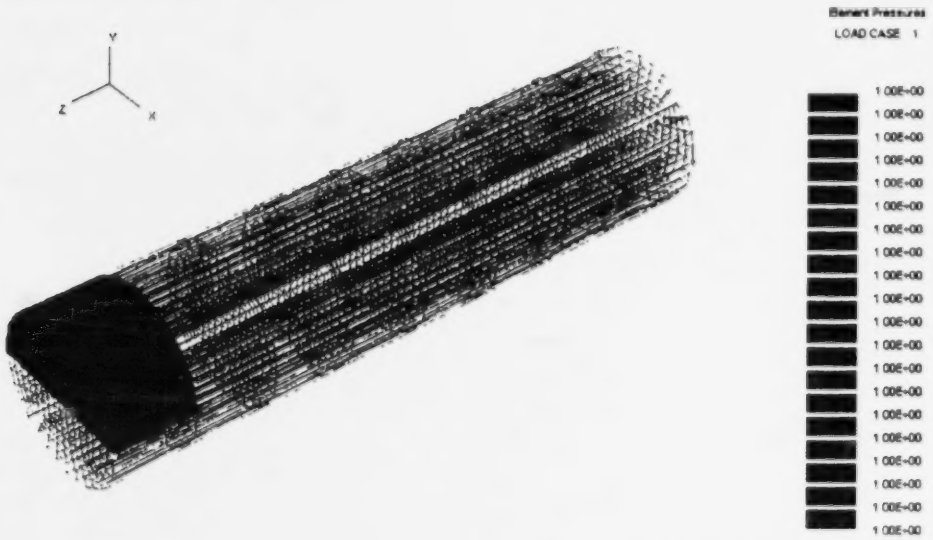

Figure 3.4 – Applied pressure loading (scale factor, $\phi = 294$)

P51700[illegible].PDF [Page: 31 of 54]

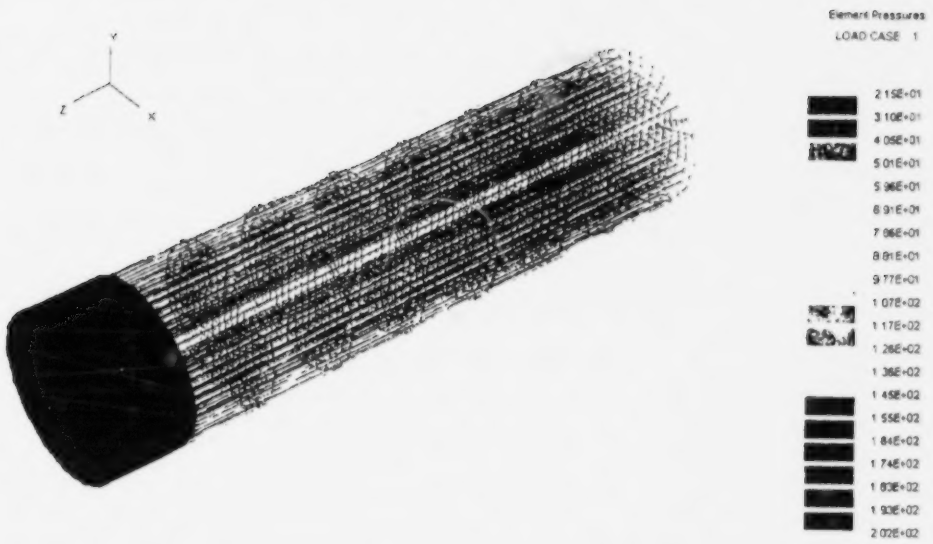

Figure 3.5 - Applied pressure loading simulating applied magnetic field and mechanical loading

4. RESULTS AND DISCUSSIONS

4.1 Specimen Response in the Absence of an Applied Magnetic Field

The first task required an assessment of the specimen response, including fracture toughness, in the absence of an applied magnetic field. As previously mentioned, specimen 4 of the data set provided by Hyatt [3] was selected for comparison with the finite element predictions. The relevant material properties and specimen data are as follows (recall Table 3.1):

- 'Zero-Field' Elastic Modulus, $E^H = 30{,}000$ MPa
- Experimental Fracture Load, $P_f = 474.6$ kg
- Load at Possible Initiation of Tensile Failure, $P_T = 254.25$ kg
- Tensile Strength, $\sigma_{T,ult} = 28$ MPa

To arrive at a suitable mesh density giving the best combination of predictive accuracy and computational efficiency, a convergence study was undertaken, in which the mesh density was successively increased in the longitudinal and circumferential directions. The successive mesh refinements are illustrated in Figure 4.1a-d (recall the fracture elements surrounding the crack tip are light orange in color). Model R0 represents the initial model discretization (i.e., no refinement), while model R1 illustrates a refined mesh in the longitudinal direction only. Model R2 shows a mesh refinement in the circumferential direction only. Finally, the mesh discretization of model R3 combines those of models R1 and R2, yielding a mesh that is refined in both the longitudinal and circumferential directions. In going from model R0 to model R3, the number of nodes and elements increased from only 1957 nodes and 384 elements to almost 14,000 nodes and over 3000 elements, respectively, with a corresponding increase in solution time of over 40 times. The results of the convergence study are summarized in Table 4.1.

From Table 4.1, it is evident that mesh refinement has little effect on the maximum axial displacement. However, circumferential mesh refinement has a much greater effect on solution convergence than does longitudinal refinement in this case, as evidenced by the changes in maximum tensile stress, back-calculated tensile failure load and stress intensity factors for all three modes. Although model R3 provides the most converged solution, the computational cost

P517007.PDF [Page: 33 of 54]

was relatively high. Therefore, it was decided that the best compromise would be the use of model R2, which offered very similar predictions at only half the computational cost of R3.

The displacement contours for lateral, vertical and axial displacements are illustrated in Figure 4.2. Vertical deflections appear to be large compared to the axial displacements, thereby suggesting that additional support may be required along the longitudinal boundaries of the specimen. The stress components in the three orthogonal directions are presented in Figure 4.3, with the corresponding VonMises stress contours provided in Figure 4.4. For clarity, the enriched crack tip elements have been removed from these contour plots. It was reported by Hyatt [3] that an inflection point existed in the load versus deflection data for specimen 4 at a load of approximately 254.25 kg. This could possibly have been an indication of tensile failure in the bottom-most fibers of the specimen at the support. Using the FE-predicted axial stresses, the allowable load prior to the onset of tensile failure was back-calculated as (28.0/88.61)x (474.6kg) = 150 kg, which represents an error on the order of approximately 41% with the value reported at the inflection point. Alternatively, the tensile strength of the specimen tested by Cunningham et al [1] could have actually been (254.25/474.6)x28 = 47.5 MPa.

Based on application of the experimental fracture load of 474.6 kg (4656 N), the mode II stress intensity factor (K_{II}) predicted for model R2 is 4.497 MPa$\sqrt{m}$. Assuming that the cracks observed during experimental testing were due to mode II fracture, then the mode II fracture toughness (K_{IIc}) may be assumed to be approximately 4.497 MPa$\sqrt{m}$, which is comparable to that of brittle materials like ceramics. The predicted mode III stress intensity factor is rather significant (2.018 MPa$\sqrt{m}$), perhaps a result of the complementary shear induced by the in-plane loading. The mode I stress intensity factor is approximately zero, as anticipated. Figure 4.5 illustrates the non-contoured variation in stress intensity factor for mode I, while the contoured plots (for all modes) are presented in Figure 4.6. For clarity, only the enriched twenty-noded fracture elements have been included in the contour plots of Figure 4.6.

4.2 Specimen Response in the Presence of an Applied Magnetic Field

The final task entailed an evaluation of the effects on specimen response, including fracture toughness, in the presence of an applied magnetic field. As previously mentioned, specimen 2 of

P517007.PDF [Page: 34 of 54]

the data set provided by Hyatt [3] was selected for comparison with the finite element predictions. Refer to Table 3.1 for a summary of the relevant material properties and loading conditions for specimen 2. Due to the level of specimen constraint inherent in the experimental testing apparatus, it was decided that the strain-free permeability (μ^S) would be most suitable to use in the calculation of magnetic field induced prestress. Recall some of the pertinent material properties and specimen data are as follows:

- 'Zero-Flux' (Constant Field) Elastic Modulus, $E^B = 60{,}000$ MPa
- Applied Current, $I = 5$ A
- Average Magnetic Field on Specimen Axis, $H = 57.6$ kA/m
  (Based on an Average Field of 144 Oe/A, where 1 Oe = 80 A/m)
- Strain-Free Permeability, $\mu^S = 4.5 \times 4\pi \times 10^{-7}$ Tm/A
- Magnetostrictive Constant, $g = 1.5 \times 10^{-8}$ T^{-1}
- Applied Compressive Prestress, $\sigma_{ps} = 21.5$ MPa
- Experimental Failure Load, $P_f = 292$ kg

The lateral, vertical and axial displacement contours for the specimen are illustrated in Figure 4.7. As observed in the previous load case, the vertical deflections are large compared to the axial displacements, again suggesting that additional support may be required along the longitudinal boundaries of the specimen. The axial stress components are provided in Figure 4.8, while the corresponding VonMises stress contours illustrated in Figure 4.9. Using the FE-predicted axial stresses, the allowable mechanically applied load corresponding to the onset of tensile failure was back-calculated as (28.0/32.07)x(292kg) = 256 kg, which is almost 71% greater than that calculated for the previous load case, in which no magnetically-induced prestress was applied.

Based on the FE results of a specimen subjected to both an experimental failure load of 292 kg (2865 N) and the presence of a 57.6 kA/m magnetic field, one can evaluate the effects of magnetostriction on fracture toughness. Recall the mode II stress intensity factor (K_{II}) predicted for model R2 under zero magnetic field was $K_{IIc}^{H} = 4.497$ MPa$\sqrt{m}$. Assuming the cracking observed during experimental testing of specimen 2 can be attributed to mode II fracture, then the mode II magnetostrictive fracture toughness (K_{IIc}^{B}) may be assumed to be approximately

P517007.PDF [Page: 35 of 54]

2.768 MPa$\sqrt{m}$, which represents a reduction of almost 39% below that predicted in the absence of a magnetic field. As was found for the previous load case, the mode III stress intensity factor is rather significant (1.242 MPa$\sqrt{m}$), possibly due to complementary shear induced by the in-plane loading. The mode I stress intensity factor is again almost zero, as anticipated. Figure 4.10 illustrates the magnetostrictive stress intensity factor contours for mode I, II, and III fracture. For clarity, only the enriched fracture elements at the crack tip have been included in the contour plots of Figure 4.10.

Table 4.1 – Summary of convergence study on FE mesh density

Parameter	-Model Identification for Mesh Refinement-			
	R0	**R1**	**R2**	**R3**
Description	No Refinement (Coarse Model)	Longitudinal Refinement Only	Circumferential Refinement Only	Longitudinal and Circumferential
Number of Nodes/Elements	1957 / 384	3753 / 768	7253/1536	13897/3072
Max. Axial Deflection (mm)	-0.312	-0.312	-0.312	-0.312
Max. Tensile Stress (MPa)	68.19	64.29	88.61	83.70
Calculated Load at Tensile Failure (kg)	194.9	206.7	150.0	158.8
Max. Compressive Stress (MPa)	-375.2	-377.4	-395.6	-401.5
Mode I SIF K_I (MPa$\sqrt{m}$)	0.010	0.040	0.011	0.009
Mode II SIF K_{II} (MPa$\sqrt{m}$)	3.890	4.100	4.497	4.323
Mode III SIF K_{III} (MPa$\sqrt{m}$)	1.590	1.620	2.018	1.982
Solution Time Required (sec)	117.3	165.6	2533	4730

P517007.PDF [Page: 37 of 54]

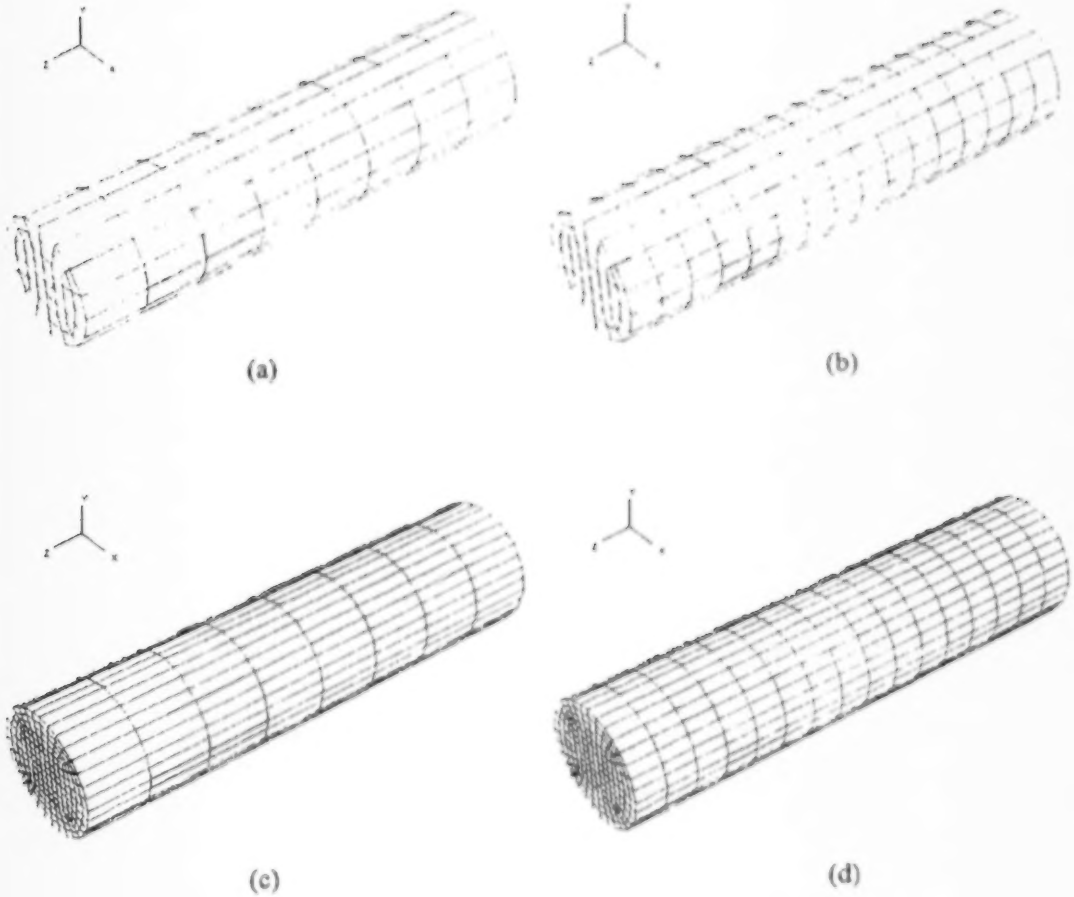

Figure 4.1 – Mesh discretization for (a) model R0, (b) model R1, (c) model R2, and (d) model R3

P517007 PDF [Page: 38 of 54]

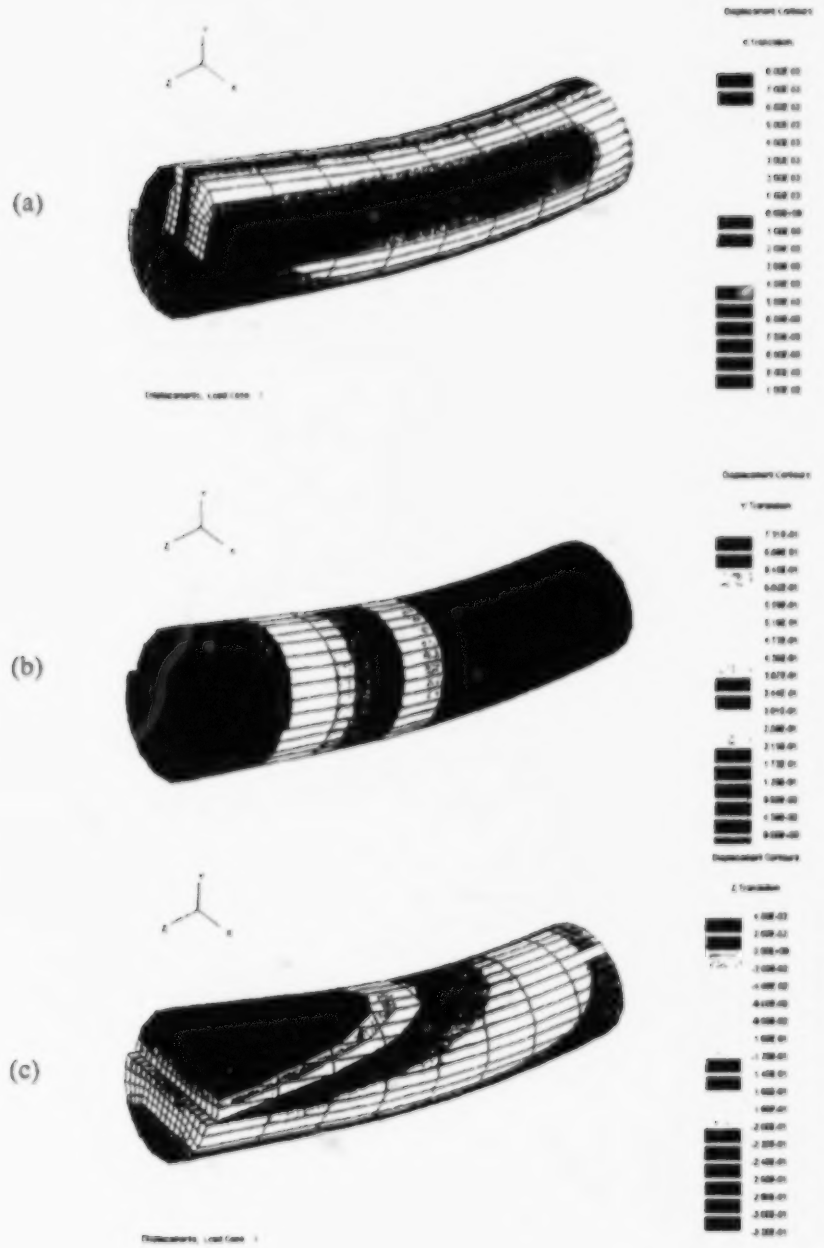

Figure 4.2 - Displacement contours for (a) X-, (b) Y-, and (c) Z-translation (no magnetic field applied)

P517007.PDF [Page: 39 of 54]

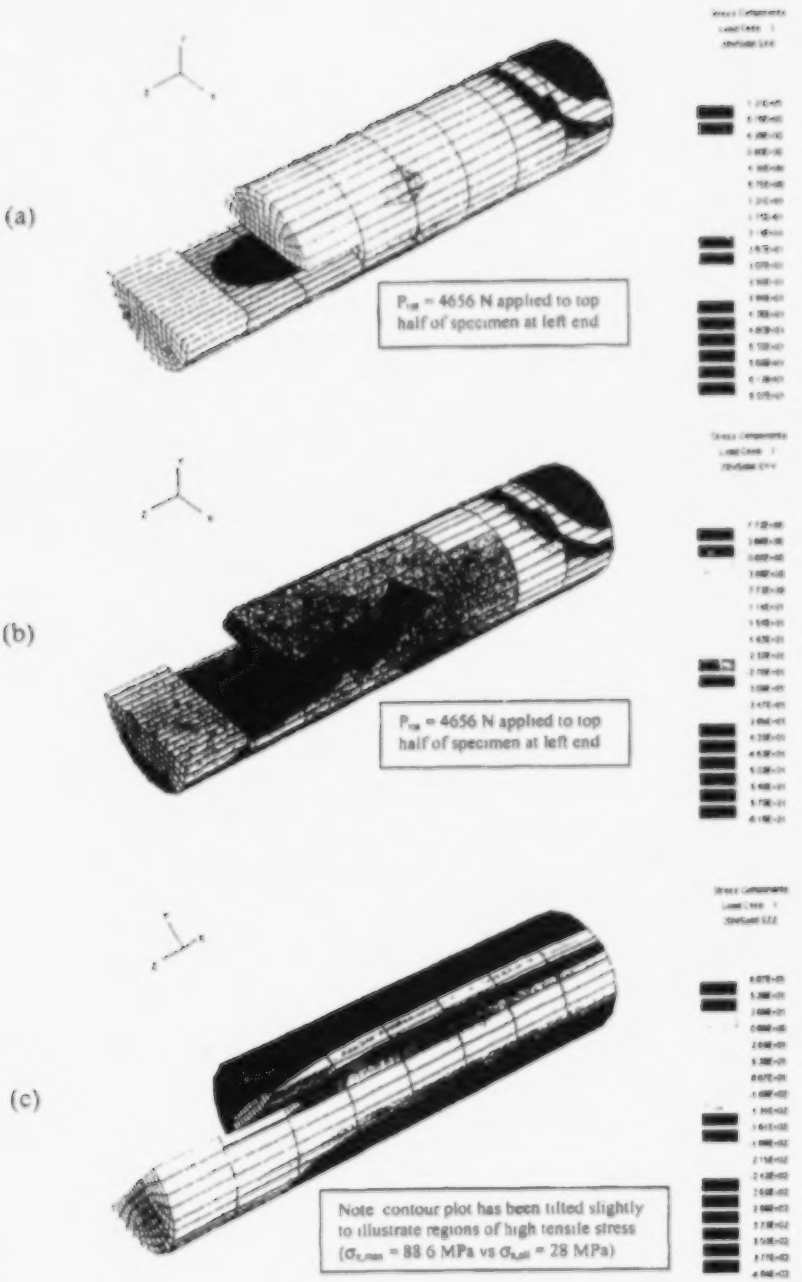
(a)
P = 4656 N applied to top half of specimen at left end
(b)
P = 4656 N applied to top half of specimen at left end
(c)
Note: contour plot has been tilted slightly to illustrate regions of high tensile stress
(σ = 88.6 MPa vs σ = 28 MPa)

Figure 4.3 - Stress components in the (a) X-direction, (b) Y-direction, and (c) Z-direction (no magnetic field applied)

P517007.PDF [Page: 40 of 54]

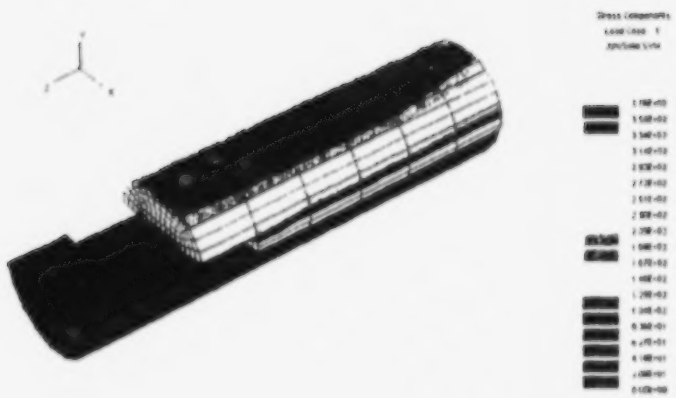

Figure 4.4 - VonMises stress contours for model R2 (no magnetic field applied)

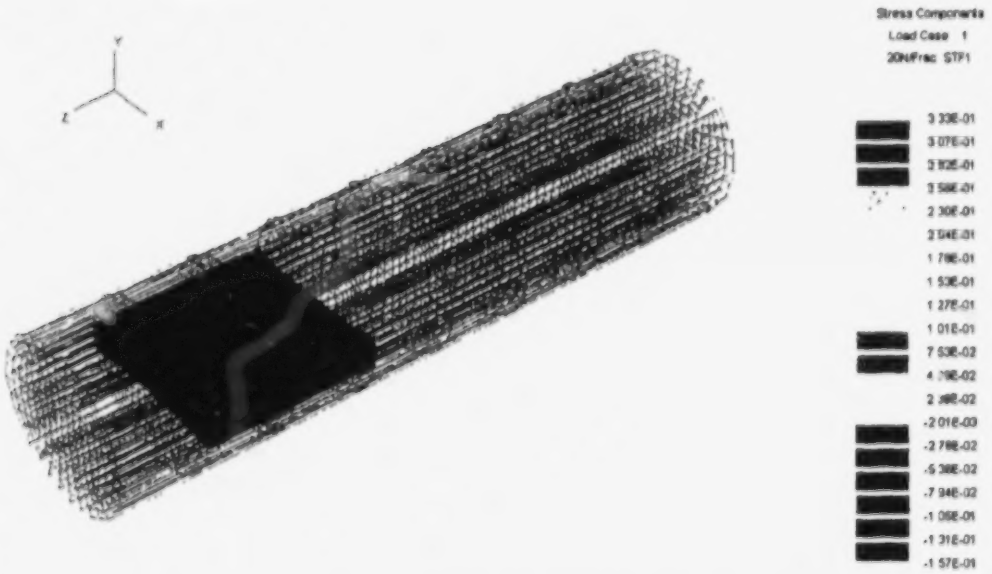

Figure 4.5 – Mode I stress intensity factor for model R2 (no magnetic field applied)

P517007.PDF [Page: 41 of 54]

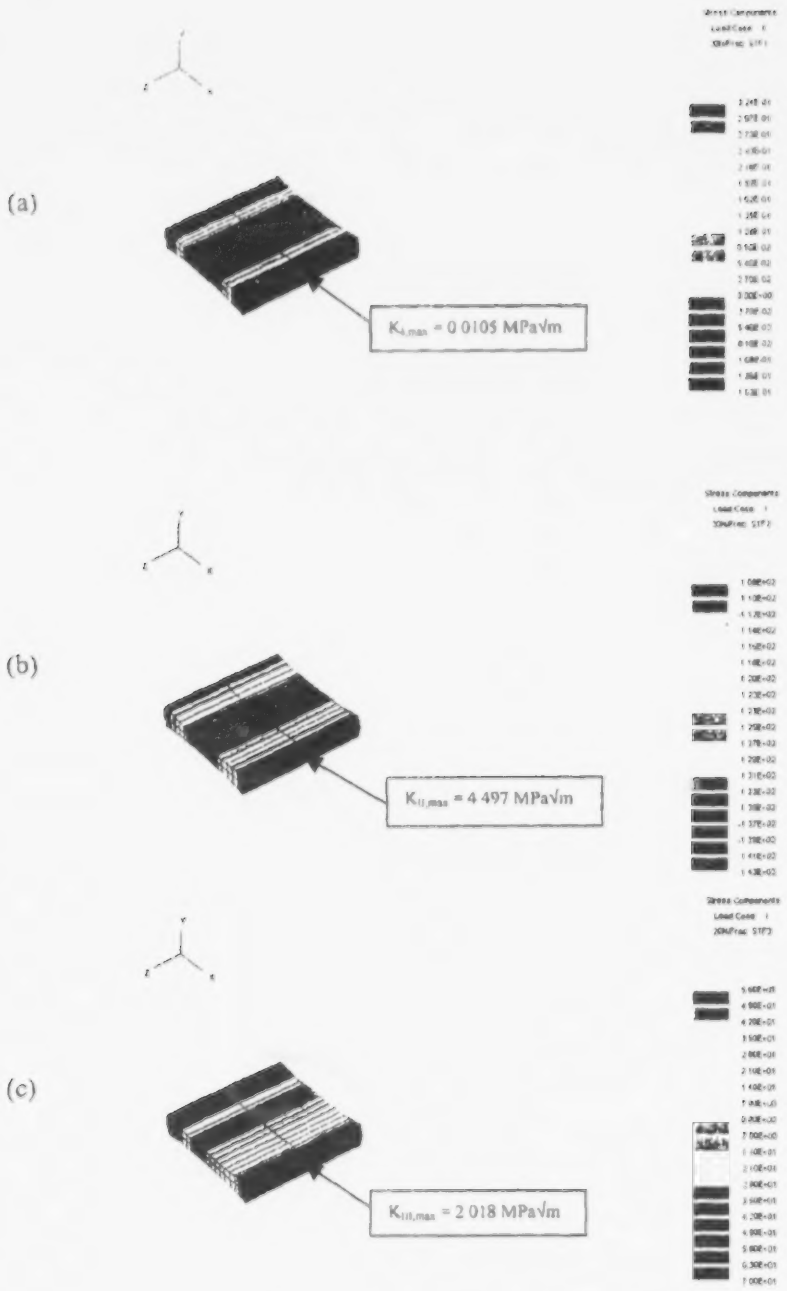

Figure 4.6 - Stress intensity factors for (a) mode I, (b) mode II, and (c) mode III fracture (no magnetic field applied, only enriched fracture elements shown)

P517007.PDF [Page: 42 of 54]

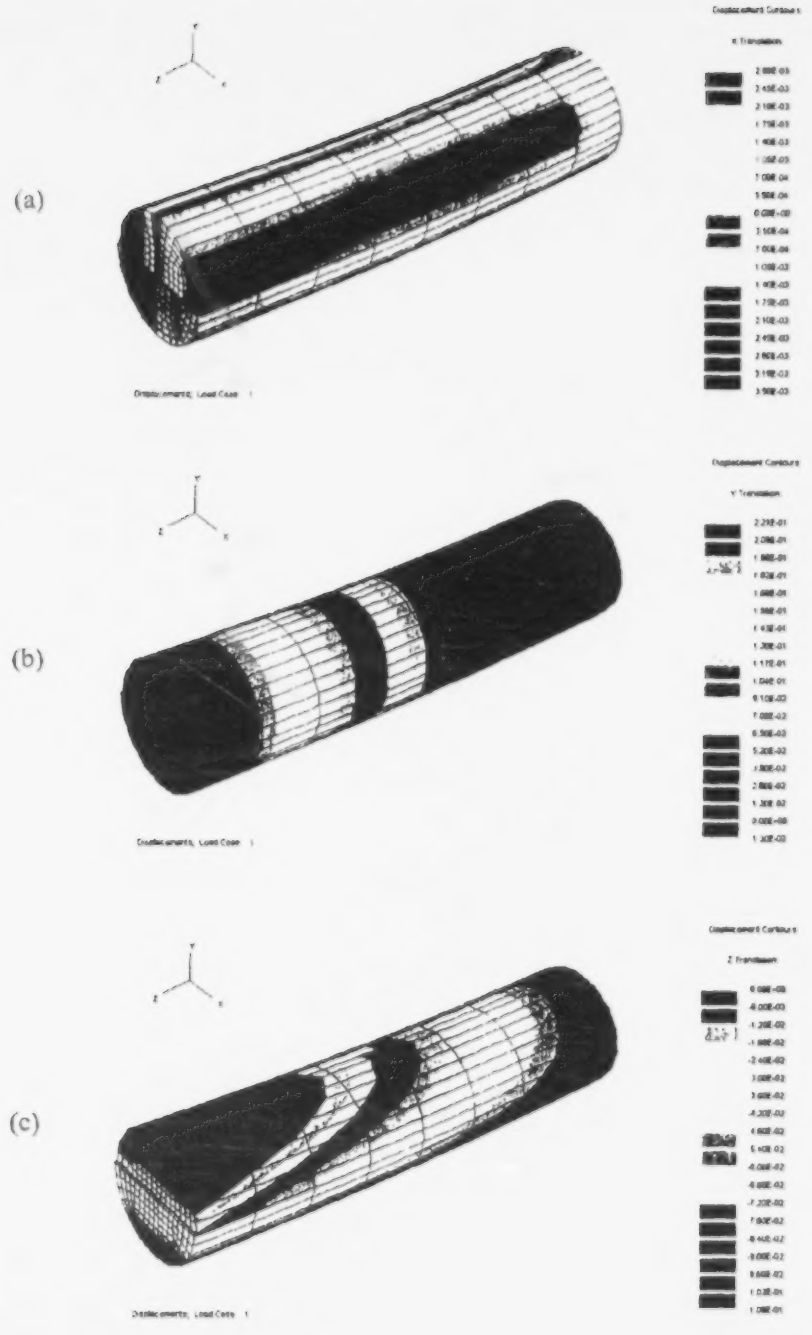

Figure 4.7 - Displacement contours for (a) X-, (b) Y-, and (c) Z-translation (57.6 kA/m magnetic field applied)

P.517007.PDF [Page: 43 of 54]

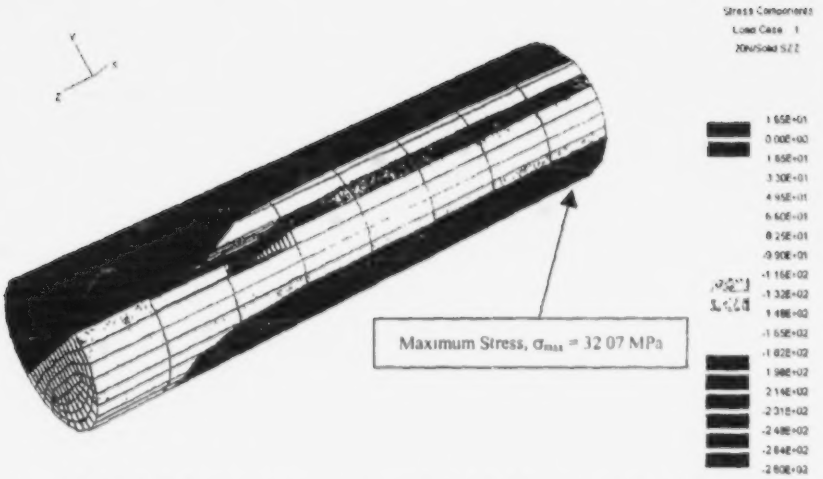

Figure 4.8 - Axial stress components (57.6 kA/m magnetic field applied)

Figure 4.9 - VonMises stress contours (57.6 kA/m magnetic field applied)

(a)

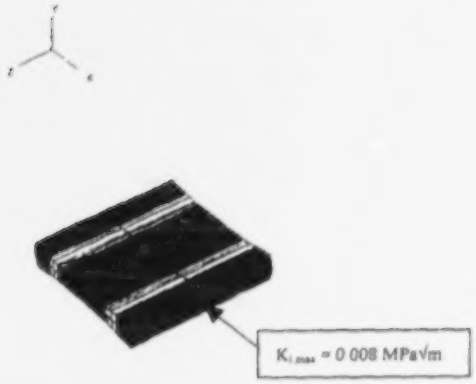
$K_{I,max}$ = 0.008 MPa√m

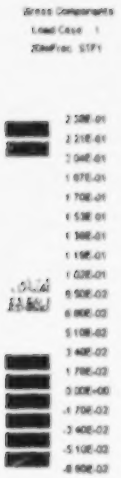
Stress Components
Load Case 1
2DefFrac STF1

(b)

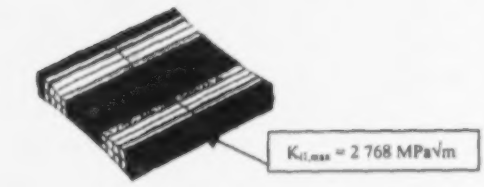
$K_{I,max}$ = 2.768 MPa√m

Stress Components
Load Case 1
2DefFrac STF2

(c)

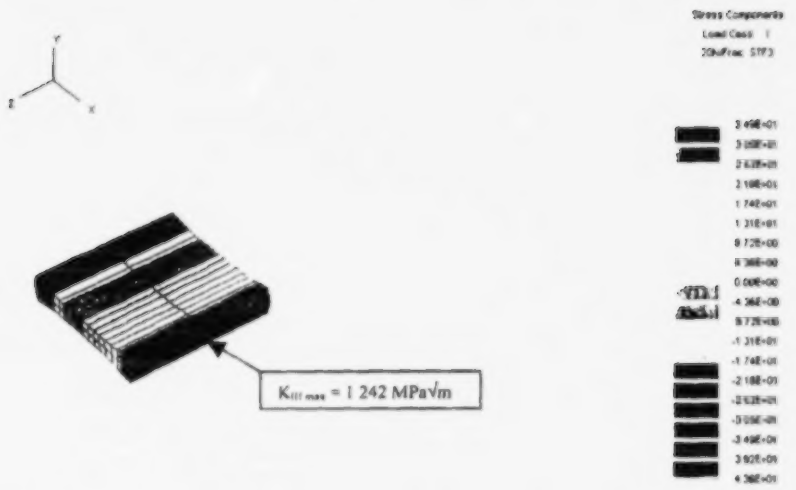

Figure 4.10 – Magnetostrictive stress intensity factors for (a) Mode I, (b) Mode II, and (c) Mode III fracture (57.6 kA/m magnetic field applied, only enriched fracture elements shown)

P517007.PDF [Page: 46 of 54]

5. SUMMARY, CONCLUSIONS, AND RECOMMENDATIONS

5.1 Summary and Conclusions

Magnetostrictive materials such as Etrema Terfenol-D are classified as smart materials, such that when subjected to a magnetic field, internal strains are induced, and conversely, when subjected to mechanical strains, a magnetic field is induced, surrounding the material. The most limiting factor hindering the use of magnetostrictive materials lies in their inherent brittleness.

For the current study, the DSA-VAST finite element software has been employed in an effort to support previous experimental investigations by Cunningham et al [1], thereby assisting in the assessment of mode II fracture toughness for magnetostrictive materials. A finite element model comprised of both conventional twenty-noded solid elements and DSA's enriched twenty-noded solid fracture element was used to model the experimental test specimen used by Cunningham et al [1].

A convergence study was performed to determine a suitable mesh discretization. It was found that the FE predictions were affected much more by mesh refinement in the circumferential direction than in the longitudinal direction. The final mesh was selected based on the optimum combination of predictive accuracy and computational efficiency.

Two load cases were investigated, namely load case 1 and load case 2. In load case 1, the magnetostrictive specimen was subjected to a mechanical load of 4656 N, equal to the experimental fracture load obtained by Cunningham et al [1] with no applied magnetic field. On the other hand, load case 2 saw the specimen subjected to both a mechanical load of 2865 N and a magnetic field of 57.6 kA/m, both corresponding to experimental failure observed by Cunningham et al [1].

From load case 1, the mode II fracture toughness was found to be approximately 4.497 MPa$\sqrt{m}$, which is very similar to values reported in the literature for materials such as ceramics. The corresponding mode II stress intensity factor was found to be rather significant at 2.018 MPa$\sqrt{m}$. Hyatt [3] also reported that during experimental testing by Cunningham et al [1], a point of inflection was observed in the load-deflection data at a load of approximately 254.25 kg. Due to the bending induced as a result of the unsymmetrical loading, it was thought that this

P517007.PDF [Page: 47 of 54]

anomaly could have been an indication of the onset of tensile failure in the bottom-most fibers of the specimen at the unnotched end. Using the FE predicted axial stresses, the allowable load prior to the onset of tensile failure was back-calculated (based on a tensile strength of 28 MPa) to be 150 kg.

For load case 2, the applied magnetic field was simulated by means of an equivalent compressive prestress applied over the entire cross section of the specimen at one end. The magnitude of this prestress (21.5 MPa) was determined based on the magnetostrictive properties for Etrema Terfenol-D. Using the FE predicted axial stresses, the allowable load prior to the onset of tensile failure was back-calculated (based on a tensile strength of 28 MPa) to be 256 kg, a value much greater than that reported for load case 1 due to the additional applied compressive prestress. The resulting mode II fracture toughness for load case 2 was found to be 2.768 MPa$\sqrt{m}$, a 39% reduction from the value reported for load case1, in which there was no magnetic field applied. The linear elastic finite element results obtained for each load case have been summarized in Table 5.1.

5.2 Recommendations

Pure mode II fracture is a result of in-plane translation only (axial in this case). However, in both load cases, it was found that the out-of-plane displacements were more than twice the axial displacements, thereby suggesting that additional support may be required along the longitudinal boundaries of the specimen in order to attain a more accurate assessment of mode II fracture toughness. A future investigation could be performed to assess the effect of additional restraint on the stress intensity factors for all fracture modes, as well as the degree of restraint required to yield near-zero values for mode I and III stress intensity factors.

In the present study, for the case of an applied magnetic field in addition to a mechanically applied load, the elastic and magnetostrictive properties of the specimen were taken as that for short-circuit conditions (that is, E^B, d, etc.). However, as Clark and Savage [4] have shown, the properties of the magnetostrictive material largely depend on the magnitude of the applied prestress. Thus, in a future investigation, it would be interesting to account for this behavior, and its effect on the mode II fracture toughness.

P517007.PDF [Page: 48 of 54]

Finally, recall that fully coupled nonlinear material behavior was not investigated during this preliminary investigation. Therefore, the ultimate goal of future investigations should involve consideration of this highly complex behavior.

P51/007 PDF [Page: 49 of 54]

Table 5.1 – Summary of results from linear elastic FE analysis

Description	Specimen 4 (No Field)	Specimen 2 (H_{ext}=57.6 kA/m)
'Zero Field' Elastic Modulus, E^H (MPa)	30,000	N/A
'Zero Flux' Elastic Modulus, E^B (MPa)	N/A	60,000
Applied Electric Current, I (A)	N/A	5
Applied Magnetic Field, H (kA/m)	N/A	57.6
Experimental Fracture Load (kg)	494.6	292
Load at Possible Tensile Failure at Support (kg)	254.25	N/A
Tensile Strength (MPa)	28	28
Compressive Strength (MPa)	700	700
Maximum Vertical Deflection, δ_y (mm)	+0.790	+0.243
Maximum Axial Deflection, δ_z (mm)	- 0.312	- 0.105
Maximum Compressive Stress (MPa)	-395.6	-265.9
Maximum Tensile Stress (MPa)	+88.61	+32.07
Maximum Allowable Load for Tensile Failure (kg)	+150	+256
Mode I Stress Intensity Factor, K_I (MPa$\sqrt{m}$)	0.011	0.008
Mode II Stress Intensity Factor, K_{II} (MPa$\sqrt{m}$)	4.497	2.768
Mode III Stress Intensity Factor, K_{III} (MPa$\sqrt{m}$)	2.018	1.242

6. REFERENCES

1. Cunningham, J., Hyatt, C.V., and KarrisAllen, K.J. "Device for Assessing Fracture Toughness of Giant Magnetostrictive Materials", Rev. Sci. Instrumentation, American Institute of Physics, Vol. 65, No. 6, pp.2137-2138, 1994.

2. Butler, J.L. "Application Manual for the Design of Etrema Terfenol-D Magnetostrictive Transducers", Edge Technologies, Ames, IA, 1988.

3. Hyatt, C.V. Various Correspondences, April 2001.

4. Clark, A.E. and Savage, H.T. "Magnetostriction of Rare Earth-Fe_2 Compounds Under Compressive Stress", Journal of Magnetism and Magnetic Materials, Vol. 31-34, pp.849-851, 1983.

UNCLASSIFIED
SECURITY CLASSIFICATION OF FORM
(highest classification of Title, Abstract, Keywords)

DOCUMENT CONTROL DATA

(Security classification of title, body of abstract and indexing annotation must be entered when the overall document is classified)

1 ORIGINATOR (the name and address of the organization preparing the document. Organizations for whom the document was prepared, e g Establishment sponsoring a contractor's report, or tasking agency, are entered in section 8)

Martec Limited
400-1888 Brunswick Street
Halifax, NS

UNCLASSIFIED

3 TITLE (the complete document title as indicated on the title page Its classification should be indicated by the appropriate abbreviation (S,C,R or U) in parentheses after the title).

Computation of Fracture Toughness of Giant Magnetostrictive Material

4 AUTHORS (Last name, first name, middle initial If military, show rank, e g Doe, Maj John E)

Koko, T. S., Rushton, P. A., and Norwood, M. E.

5 DATE OF PUBLICATION (month and year of publication of document)	6a NO OF PAGES (total containing information Include Annexes, Appendices, etc)	6b NO OF REFS (total cited in document)
May 2001	42	3

7 DESCRIPTIVE NOTES (the category of the document, e g technical report, technical note or memorandum If appropriate, enter the type of report, e g interim, progress, summary, annual or final Give the inclusive dates when a specific reporting period is covered)

Contractor Report

8 SPONSORING ACTIVITY (the name of the department project office or laboratory sponsoring the research and development Include address)

Defence Research Establishment Atlantic
P.O. Box 1012
Dartmouth, NS B2Y 3Z7

9a PROJECT OR GRANT NO (if appropriate, the applicable research and development project or grant number under which the document was written Please specify whether project or grant)	9b CONTRACT NO (if appropriate, the applicable number under which the document was written)
Project 11gh43	W7707-006853/WIHAL

10a ORIGINATOR'S DOCUMENT NUMBER (the official document number by which the document is identified by the originating activity This number must be unique to this document.)	10b OTHER DOCUMENT NOs (Any other numbers which may be assigned this document either by the originator or by the sponsor)
Martec Report #TR-01-07	DREA CR 2001-090

11 DOCUMENT AVAILABILITY (any limitations on further dissemination of the document, other than those imposed by security classification)

(X) Unlimited distribution
( ) Defence departments and defence contractors; further distribution only as approved
( ) Defence departments and Canadian defence contractors; further distribution only as approved
( ) Government departments and agencies; further distribution only as approved
( ) Defence departments; further distribution only as approved
( ) Other (please specify): Informal publication in draft format only for limited distribution

12 DOCUMENT ANNOUNCEMENT (any limitation to the bibliographic announcement of this document This will normally correspond to the Document Availability (11). However, where further distribution (beyond the audience specified in (11) is possible, a wider announcement audience may be selected).

Full Unlimited

UNCLASSIFIED

DCD03 2/06/87-M/ DREA mod 17 Dec 1997

13. ABSTRACT (a brief and factual summary of the document. It may also appear elsewhere in the body of the document itself. It is highly desirable that the abstract of classified documents be unclassified. Each paragraph of the abstract shall begin with an indication of the security classification of the information in the paragraph (unless the document itself is unclassified) represented as (S), (C), (R), or (U). It is not necessary to include here abstracts in both official languages unless the text is bilingual)

Magnetostrictive materials such as Etrema Terfenol-D are classified as smart materials, which, when subjected to a magnetic field, experience internal strains, and conversely, when subjected to mechanical strains, experience a magnetic field. The most limiting factor impeding the use of magnetostrictive materials lies in their inherent susceptibility to brittle fracture. Previous studies at DREA have led to the development of a new mechanical device for mode II fracture testing of magnetostrictive materials in the presence or absence of a magnetic field. The test specimen is cylindrical in shape, 6.35 mm in diameter, 25.4 mm in length, with a 20 μm wide EDM notch extending through its diameter for a distance of 6.35 mm along its length. The present study applies finite element technology to support these experimental investigations, thereby lending assistance in the assessment of mode II fracture toughness for magnetostrictive materials. This is an initial exploratory effort, in which the fully coupled non-linear behavior of the material is not considered. Rather, a methodology for converting the applied magnetic field to an equivalent mechanical load, based on the material's magnetostrictive properties, is devised and applied.

The DSA-VAST finite element software was employed to produce a model comprised of conventional solid elements, and also featuring DSA's enriched twenty-noded solid fracture element. Two load cases were investigated, namely one in which a mechanical load was applied to the specimen in the absence of a magnetic field, and a second case in which a magnetic field was applied to the specimen in addition to a mechanical load. In the absence of an applied magnetic field, the mode II fracture toughness was found to be approximately 4.497 MPa$\sqrt{m}$, which is in the range of values reported for ceramic-like materials. On the other hand, in the presence of an applied magnetic field (simulated by an equivalent compressive prestress), the resulting mode II fracture toughness was found to be 2.768 MPa$\sqrt{m}$, a 39% reduction from the corresponding 'zero-field' value. In each laod case, the out-of-plane displacements were more than twice the axial displacements, thereby suggesting that additional support be placed along the longitudinal boundaries of the specimen in order to attain a more accurate assessment of mode II fracture toughness.

14. KEYWORDS, DESCRIPTORS or IDENTIFIERS (technically meaningful terms or short phrases that characterize a document and could be helpful in cataloguing the document. They should be selected so that no security classification is required. Identifiers, such as equipment model designation, trade name, military project code name, geographic location may also be included. If possible keywords should be selected from a published thesaurus, e.g. Thesaurus of Engineering and Scientific Terms (TEST) and that thesaurus identified. If it not possible to select indexing terms which are Unclassified, the classification of each should be indicated as with the title)

Toughness, Terfenol, Magnetostrictive, Finite Element

UNCLASSIFIED
SECURITY CLASSIFICATION OF FORM